DIRECT NUMERICAL SIMULATION OF TURBULENT BOUNDARY LAYER OVER SPARSELY SPACED ROD ROUGHENED WALL

Muhammad Nadeem, Jae Hwa Lee and Hyung Jin Sung*
Department of Mechanical Engineering, KAIST
291 Daehak-ro, Yuseong-gu, Daejeon 305-701, Korea
mnadeem@kaist.ac.kr, jhlee06@kaist.ac.kr, hjsung@kaist.ac.kr

ABSTRACT

Direct Direct numerical simulations (DNSs) of spatially developing turbulent boundary layers (TBLs) over 2D rod-roughened walls were performed to investigate the structure of TBL over the sparsely distributed roughness element. 2D rod elements were employed periodically arranged in the streamwise direction with pitches of p_x/k = 8, 16, 32, 64 and 128, where p_x the streamwise spacing of the roughness and k is the roughness height. The frontal solidity (λ_f) of the present study ranges from 0.125 to 0.0078 that corresponds to the sparse distribution regime ($\lambda_f < 0.15$). The Reynolds number based on the momentum thickness was varied in the range Re_θ = 300~1400 and the roughness height was $k = 1.5\theta_{in}$, where θ_{in} is the momentum thickness at the inlet. The characteristics of the TBLs such as friction velocity, mean velocity and Reynolds stresses over the 2D rod-roughened walls were compared with the result from TBL over a smooth wall at the similar Reynolds number. The amplitude modulation analysis was performed to study the inner/outer layer interaction of TBL. It was shown that the interaction between the inner and outer layers is maximum for the case of p_x/k = 8, the rough wall flows support the Townsend's wall similarity hypothesis.

INTRODUCTION

For several decades, the study of turbulent boundary layers over rough walls has been an important subject, since majority of the flows encountered in engineering applications often interact with surface roughness elements. The surface roughness in general increases drag and effects on the characteristics of heat, mass and momentum transfer and is also very important in meteorological flows in the form of buildings and vegetation canopies. Furthermore, the introduction of the roughness to surface triggers transition of flow from laminar to turbulent states. Therefore, the understanding of structure over rough wall flows will serve the information for better control and design of engineering equipment with contribution to the fundamental turbulence research.

The review articles of Raupach et al. (1991), Jiménez (2004) and Flack and Shultz (2010) have comprehensively summarized the wall bounded flows with a large range of roughness surfaces. These reviews support the wall similarity hypothesis of Townsend (1976), which states that outside the roughness sublayer turbulent motions are independent of the surface roughness and that the interaction between the inner and outer layers is very weak at sufficiently large Reynolds numbers. Furthermore outside the roughness sublayer, both the defect form and turbulent stresses normalized by a friction velocity are unaffected by surface roughness. A number of studies have shown support for Townsend's wall similarity hypothesis for a large range of 3D roughness types and sizes. These include the work of Flack et al. (2005) for sandpaper and mesh, Shockling et al. (2006) for a honed pipe, Schultz and Flack (2007) for a scratched surface. Similarity has also been observed to exist for large 3D roughness as demonstrated by Castro (2007) for mesh, staggered cubes and gravel chips with k/δ < 1/10 for the largest roughness, and by Flack et al., (2007) for mesh and sandpaper with k/δ < 1/16 (δ is boundary layer thickness). Volino et al. (2009) showed outer-layer similarity between cases with 3D roughness and smooth walls.

On the other hand, previous studies of TBL flows over 2D rough wall have shown the contradicting behavior to the wall similarity hypothesis. Krogstad and Antonia (1999) carried out measurements for a transverse rod roughness of p_x/k = 4 (where p_x is the streamwise spacing of the cubes) and showed that there is an increase in the Reynolds stress profiles in the outer layer compared with those over a smooth wall. Similar results were found in the direct numerical simulation (DNS) study of Lee and Sung (2007). Djenidi et al. (2008) conducted experiments with 2D transverse square bars with p_x/k ranging from 8 to 16 and showed that the roughness function was greatest for p_x/k = 8, although the largest effect on the Reynolds stresses occurred for p_x/k = 16. Volino et al. (2009) conducted experiments with transverse square bars with p_x/k = 8. They reported an increase in the Reynolds stresses in the outer layer for the 2D bars compared to smooth wall cases. Krogstad et al. (2005) considered a turbulent channel flow with 2D bar both experimentally and numerically, and showed no roughness effects on the outer layer. It was suggested that channel flows respond differently to roughness than boundary layer flows possibly due to the difference in the outer boundary condition.

More recently, DNS study of TBL over cube roughened wall with streamwise and spanwise pitch of p_x/k = 8 and p_z/k = 2 in staggered array was performed by Lee et al. (2011). They showed that the Reynolds stresses affects the outer layer. Volino et al. (2011) also conducted the experimental study with 2D bar and 3D cube in staggered arrangement, and showed the similar results. However, Krogstad and Afros (2012) conducted experiments with 2D rod roughness at higher Reynolds number, and showed that Townsend's wall similarity is established, because the discrepancy of the Reynolds stresses is reduced at this Reynolds number. Further, to investigate the effect of roughness element spacing, Lee et al. (2012) performed a DNS study over rod and cube roughened walls with p_x/k = 2, 3, 4, 6, 8, and 10 with spanwise extent fixed at p_z/k = 2. They showed that the

Reynolds stress in outer layer increases in proportional to p_x/k for both flows.

The objective of the present study is to investigate the interaction between inner and outer layers in TBL over sparsely distributed rough walls. For this purpose, a number of DNSs of TBLs over rod-roughened wall were carried out with p_x/k = 8, 16, 32, 64, and 128. The frontal solidity (λ_f) of the present study, which is the ratio of frontal area of the roughness element per unit wall parallel area, ranges from 0.125 to 0.0078 that corresponds to the sparse distribution regime (λ_f < 0.15). The streamwise domain size is varied from $768\theta_{in}$ to $1536\theta_{in}$ so that flow may achieve a new equilibrium position after the initial step change. The characteristics of TBL such as mean velocity, velocity defect, roughness function and Reynolds stresses were obtained and compared with those of smooth wall. Further, to analyze the interaction of inner and outer layers, two-point amplitude modulation covariance was determined for all cases.

NUMERICAL DETAILS

For an incompressible flow, the non-dimensional governing equations are

$$\frac{\partial u_i}{\partial t}+\frac{\partial u_i u_j}{\partial x_j}=-\frac{\partial p}{\partial x_i}+\frac{1}{\mathrm{Re}}\frac{\partial^2 u_i}{\partial x_j \partial x_j}+f_i \qquad (1)$$

$$\frac{\partial u_i}{\partial x_i}=0 \qquad (2)$$

where the x_i are the Cartesian coordinates and the u_i are the corresponding velocity components. All variables are nondimensionalized by the free-stream velocity (U_∞) and the momentum thickness at the inlet (θ_{in}), and the momentum thickness Reynolds number is defined as $Re_\theta = U_\infty\theta_{\mathrm{in}}/\nu$, where ν is the kinematic viscosity. The governing equations are first integrated in time by using the fractional-step method with the implicit velocity-decoupling procedure proposed by Kim et al. (2002). On the basis of a block LU decomposition, both the velocity pressure decoupling and the additional decoupling of intermediate velocity components are achieved through approximate factorization. The immersed boundary method was used to describe the roughness elements with Cartesian coordinates and a rectangular domain (Kim et al., 2001). Details regarding the numerical algorithm can be found in Lee and Sung (2007).

The notational convention adopted is that x, y, and z denote the streamwise, vertical, and spanwise coordinates, respectively, and that u, v, and w denote the streamwise, wall-normal, and spanwise components of the velocity fluctuations. Figure 1 shows a schematic diagram of the small portion of computational domain for flow over 2D rod roughened-wall for p_x/k = 8, 16, and 32. Six main simulations, including five 2D rough wall conditions and the smooth wall condition, were performed. The five 2D rough wall conditions were formed by varying the streamwise spacing over the values p_x/k = 8, 16, 32, 64 and 128. The first rod was placed at distance of $80\theta_{in}$ downstream from the inlet; the surface conditions at this point changes abruptly from smooth to rough wall, which is

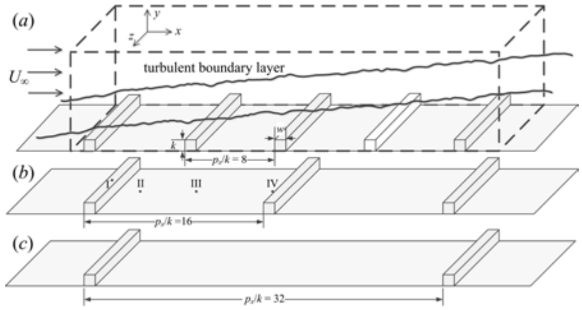

Figure1. Schematic diagram of computational domain and of 2D rough wall with different value of p_x/k.
(a) px/k = 8, (b) p_x/k =16, (c) p_x/k =32

defined as x = 0. This inflow data over the smooth wall at Re_θ = 300 was obtained by the auxiliary simulations based on the method of Lund et al. (1998). Therefore, the domain size should be sufficiently long for the flow to reach a new equilibrium state, which results in self-preservation in the computational domain. These domain sizes were confirmed to be adequate by verifying the convergence of the two-point correlation to zero for half of the present computational domain in the streamwise and spanwise directions. At the exit, the convective boundary condition was specified as $(\partial u/\partial t) + c(\partial u/\partial x) = 0$, where c is the local bulk velocity. The no-slip boundary condition was imposed at the solid wall, and the boundary conditions on the top surface of the computational domain were $u = U_\infty$ and $\partial v/\partial y = \partial w/\partial y = 0$.

Four locations, indicated as I, II, III or IV in figure 1(b) were chosen to examine the variation of turbulent statistics along the wall-normal distance from the wall. Location I is placed at the centre of the roughness crest and location II is near the focal point of the first recirculation zone. Location III is the geometric centre of the two adjacent roughness elements in the streamwise direction. Finally, location IV is placed in front of the leading edge of roughness element. In the following sections, the turbulent statistics in the inner and outer layers were obtained at location III, with $\delta/\theta_{in} \approx 30$ and comparable $\mathrm{Re}_\theta \approx 1350$ to highlight the influences of the streamwise spacing.

RESULTS AND DISCUSSION

To investigate the interaction between the inner and outer layers of the turbulent boundary layer over sparsely spaced 2D rough walls, mean velocity, Reynolds stress profiles are obtained and compared with those of smooth wall flow. Further the amplitude modulation analysis was carried out. The results are discussed in the following sub-sections.

Mean Velocity

Figure 2 shows the profiles of mean velocity and velocity defect form at location II for p_x/k = 8 to 128. The profile of the smooth wall agreed well with the standard law of the wall; however, the mean velocities of rough walls were all shifted downward due to the roughness effect. The extent of this shift (roughness function ΔU^+) is maximum at

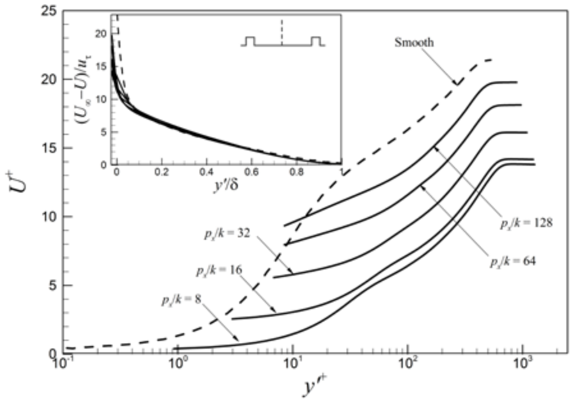

Figure 2.Mean streamwise velocity profiles and mean velocity defect profiles (inset) for 2D rough walls with p_x/k = 8 to 128

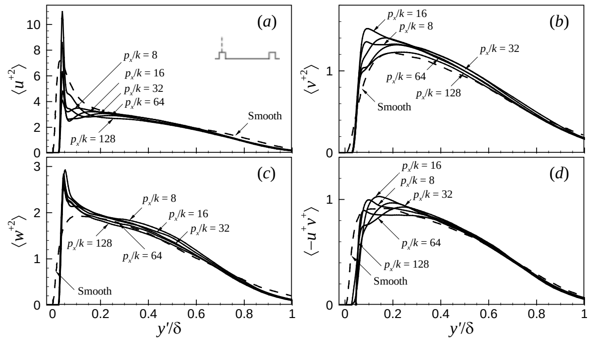

Figure 3. Reynolds stresses in the outer coordinates at center of two roughness elements for flows over 2D rough walls with p_x/k = 8 to 128

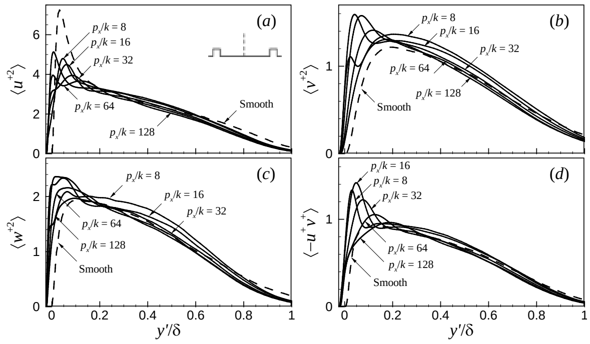

Figure 4. Reynolds stresses in the outer coordinates at center of two roughness elements for flows over 2D rough walls with p_x/k = 8 to 128

p_x/k = 8 which is consistent with the drag coefficient and the friction velocity. This suggests that the roughness function derived from the mean velocity profile in the log layer is closely associated with the wall-friction parameters, especially the friction velocity. As expected, the roughness function value, ΔU^+ decreases with increasing the roughness spacing, indicating the reduced effect of roughness elements. Note that the roughness Reynolds number k_s^+ is obtained from the following relation to the roughness function, as described by Raupach *et al.* (1991). The values of k_s^+ exceeds 40 for p_x/k = 8 to 32, whereas k^+ is more than 10 for all values of p_x/k indicating that the present rough-wall TBLs fall under the fully rough regime. The distributions of the velocity defect form along the outer coordinate are found to collapse in the outer region, indicating that the outer mean flow is less sensitive than the inner mean flow, supporting the outer layer wall similarity.

Reynolds Stresses

Figure 3 and 4 show the Reynolds stress profiles over rod roughened walls with p_x/k = 8 to 128 at the centre of the roughness crest (location I) and at the centre of two adjacent roughness elements (location III) respectively. The Reynolds stress data of flow over smooth wall is also included for comparison.

In figure 3(a), the streamwise normal stresses, $\langle u'^2 \rangle$ have a peak at y'/δ = 0.5 and the peak s increases with increasing the roughness spacing. Further, these profiles collapse to the smooth wall profile beyond y'/δ = 0.25. The wall normal stresses, $\langle v'^2 \rangle$ (figure 3*b*) are considerably higher for all rough wall cases than the smooth wall. The spanwise normal stresses and Reynolds shear stresses exhibit a similar behavior. The maximum contribution to the wall normal and Reynolds shear stresses in the inner region occurs at p_x/k = 16 with peak location existing at y'/δ = 0.1 and y'/δ = 0.15, respectively. Moreover, the Reynolds shear stresses are higher in the outer region for p_x/k = 16 as compared to p_x/k =8, which is consistent with the findings of Djenidi et al. (2008).

For the streamwise normal stresses, $\langle u'^2 \rangle$, the inner peak values are shown to be decreased from p_x/k = 8 to p_x/k = 32 and then increased for p_x/k > 32. This indicates that the effect of roughness element is increased up to p_x/k = 32 and is decreased for p_x/k > 32. In the outer layer, the profiles for p_x/k = 8 and 16 are found to be different from that over the smooth wall. However, for $p_x/k \geq 32$ these profiles collapse well with the smooth-wall profile, indicating the little interaction between the inner and outer layers. The Reynolds shear stresses increase with increasing the roughness spacing with a maximum value at p_x/k = 16 and then decreases, similar to the streamwise normal stress. The consistent result is observed for the wall-normal stresses $\langle v'^2 \rangle$ in the outer layer. Djenidi et al. (2008) showed that the Reynolds stresses of p_x/k = 16 normalized by the wall unit are higher than those of p_x/k = 8 in the outer region. However, in this study it is found that the Reynolds stresses for p_x/k = 16 are higher within the region of y'/δ = 0.15, and beyond this point the Reynolds stresses are higher for p_x/k = 8. The higher values of Reynolds stresses in the inner region may be attributed to the reattachment of flow to the wall in TBL. These finding suggest that for p_x/k = 32, the TBL over the rod roughened wall supports the Townsend's wall similarity hypothesis.

Amplitude Modulation

The interaction between the inner and outer layers of the TBL can be studied by the effect of the large scale motions present in the outer layer on near wall structures in the inner

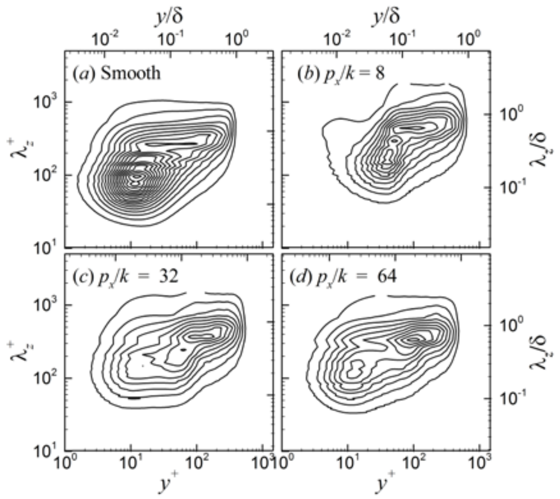

Figure 5. Pre-multiplied spanwise spectra of streamwise velocity fluctuations. Data are scaled with u_τ^2 and minimum contour level is 0.02 and increment is in steps of 0.02.

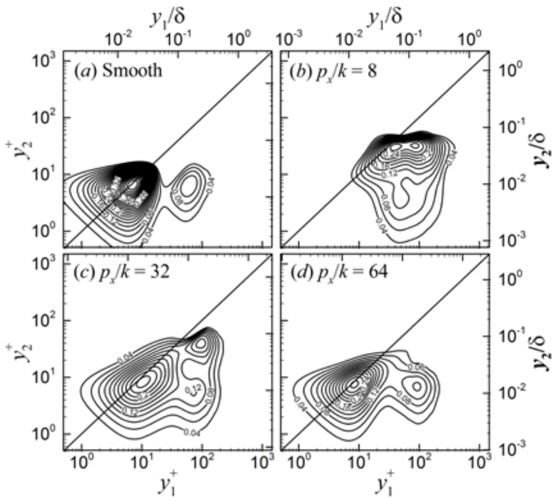

Figure 6. Two-point AM covariance for smooth and 2D rough walls

layer of the TBL. Mathis et al. (2009) quantified this interaction of large and small scales by the amplitude modulation of small scales in near wall region by the large scales in the outer layer. They employed a decoupling procedure based on the Hilbert transform of the velocity signals in turbulent boundary layers to quantify the amplitude modulation phenomena through the introduction of a one-point correlation coefficient. A note of caution concerning the interpretation of the amplitude modulation correlation coefficient is made by Schlatter and Örlü (2010) in which they demonstrated that the correlation coefficient used to quantify the amplitude modulation is proportional to the skewness of the original signal irrespective of any modulation. The analysis of Mathis et al. (2009) is extended by Bernardini and Pirozzoli (2011) using the two-point amplitude modulation (AM) correlation coefficient. They showed that this new two-point correlation does not appear to be proportional to the skewness of the original signal and therefore it provides a refined quantification of the amplitude modulation effects and truly reflects the top-down interaction.

To investigate the interaction between inner and outer layers and the effect of the surface roughness on this interaction, the method suggested by Bernardini and Pirozzoli (2011) is chosen. First of all, the pre-multiplied spanwise spectra of the streamwise velocity $k_z/\phi_{uu}(k_z)$ ($k_z = 2\pi/\lambda_z$ is the spanwise wavenumber and ϕ_{uu} is the spectral density of u with respect to the spanwise direction) are determined to investigate the secondary peak which is associated with the large scale organization of velocity fields on logarithmic region of the TBL. Then the raw velocity signal is separated into large scale component (u_L) and small scale component (u_s) using the spanwise filter wavelength chosen according to the wavelength which approximately separates the inner and outer peaks in the energy spectrum. In this study the raw signal is separated into large and small scales using the filter with cutoff wavelength $\lambda_z = 0.5\delta$. The modulating influence of large scale component at wall-normal position at y_1 on small scale component at another position y_2 is quantified by the covariance $C^{2p}(y_1, y_2) = \langle u_L(y_1)u_{EL}(y_2)\rangle$, where $u_L(y_1)$ is the large scale component at location y_1 and $u_{EL}(y_2)$ is the low-pass filtered envelope of the small-scale component of the raw signal at location y_2.

The pre-multiplied spanwise spectra of the streamwise velocity for smooth wall and for rough walls with $p_x/k = 8$, 32 and 64 are reported in figure 5. It is interesting to note that by the introduction of the rod roughness the position of the inner peak is shifted from $y^+ \approx 15$ to $y^+ \approx 40$ ($y/\delta = 0.06$) for $p_x/k = 8$. This shift of the location of inner peak shows that the inner-scaled turbulent energy of the structure over the rough wall is transferred to the outer layer, consistent with the profiles of the streamwise Reynolds stress. The spanwise length scale shifted from 100 to 200, indicating the increase of the mean spanwise distance of quasi-streamwise vortices. For $p_x/k \geq 32$, the inner peak location is shifted back to $y^+ \approx 12$. This suggests that flow over the rough wall for $p_x/k \geq 32$ is similar to that of the smooth wall.

The two-point amplitude modulation covariance contour plots for smooth and rough walls with $p_x/k = 8$ to 128 are shown in figure 6. For smooth wall, the contour lines are symmetric with respect to the diagonal line with two distinct peaks (one located at $y_1^+ = y_2^+ \approx 7{-}8$ and other $y_1^+ \approx 80-100$ and $y_2^+ \approx 7{-}8$). For rough wall flows the locations of these peaks are changed from the smooth wall and also the strength of these peaks are increased which indicates the strong interaction between inner and outer layers. For $p_x/k = 8$, the locations of the peaks move to $y_1^+ = y_2^+ \approx 35$ and at $y_1^+ \approx 80-100$ and $y_2^+ \approx 35$ and the peak value of the outer peak is about 0.26. For $p_x/k = 16$ and 32, the inner peak moves back toward the wall at $y_1^+ = y_2^+ \approx 8{-}12$ and other $y_1^+ \approx 80-100$ and $y_2^+ \approx 35$ and the strength of the outer peak is about 0.24 and 0.16 respectively. For $p_x/k \geq 32$, the plots of the two-point amplitude modulation covariance are qualitatively similar to that of the smooth wall with peaks located at $y_1^+ = y_2^+ \approx 7{-}8$ and other $y_1^+ \approx 80-100$ and $y_2^+ \approx 7{-}8$. This is an indicator of the similarity of the rough wall flows to the smooth wall flows.

SUMMARY AND CONCLUSIONS

In the present study, DNS of spatially developing TBLs over 2D rod-roughened walls were performed to investigate the structure of TBL over the sparsely distributed roughness element and the results were compared with the previous studies. The main emphasis was placed on the interaction between inner and outer layers of TBL. The values of roughness element spacing in the streamwise direction that were used in this study are p_x/k = 8, 16, 32, 64 and 128 which gives the frontal solidity (λ_f) ranging from 0.125 to 0.0078 which lies in a sparse distribution regime ($\lambda_f < 0.15$). The form drag, the friction velocity, and the roughness function for the flows over the 2D rough walls showed that these quantities are strongly dependent on p_x/k and that the maximum and minimum values occur at p_x/k = 8 and 128, respectively. The growth rate of turbulent boundary layer thickness (δ) and momentum thickness (θ) is larger as compared to smooth wall. This rate of growth decreases as the roughness spacing increases. The roughness sublayer is estimated to be about y=5k for all values of roughness spacing. The Reynolds stress profiles over the rod roughened walls show that the effects of roughness elements extend to the outer layer for p_x/k = 8 and 16. The wall normal stresses and shear stress are observed to be higher for p_x/k =16 within the range of y'/δ = 0.15 and in outer region the highest value is for p_x/k =8. The Reynolds stress profiles seem to collapse on the smooth wall profiles for $p_x/k \geq 32$ in conformity with Townsend's hypothesis. Finally, the effect of roughness spacing was examined on the two-point AM covariance of small scales present near the wall by the large scales present in outer region. It was observed that the introduction of roughness elements changes the energy distribution in the near wall region. The maximum change is observed for p_x/k =8. This can be confirmed from the contour plots of two-point AM covariance which shows the similar behavior. Furthermore, for $p_x/k \geq 32$, the plots of the two-point amplitude modulation covariance are qualitatively similar to that of the smooth wall which is an indicator of the validity of Townsend's similarity hypothesis.

ACKNOWLEDGEMENT

This work was supported by the Creative Research Initiatives (No. 2013-0003364) program of the National Research Foundation of Korea and partially supported by KISTI under the Strategic Supercomputing Support Program.

REFERENCES

Bernardini, M., and Pirozzoli, S., 2011, "Inner/outer layer interactions in turbulent boundary layers: a refined measure for the large-scale amplitude modulation mechanism", *Physics of Fluids,* Vol. 23 (6), pp. 061701.

Castro, I. P., 2007, "Rough-wall boundary layers: mean flow universality", *Journal of Fluid Mechanics,* Vol. 585, pp. 469–485.

Djenidi, L., Antonia, R. A., Amielh, M., and Anselmet, F., 2008, "A turbulent boundary layer over a two-dimensional rough wall", *Experiments in Fluids,* Vol. 44, pp. 37–47.

Flack, K. A., and Schultz, M. P., 2010, "Review of hydraulic roughness scales in the fully rough regime", *Journal of Fluids Engineering*, Vol. 132, pp. 041203.

Flack, K. A., Schultz, M. P., and Connelly, J. S., 2007, "Examination of a critical roughness height for boundary layer similarity", *Physics of Fluids,* Vol. 19, pp. 095104.

Flack, K. A., Schultz, M. P., and Shapiro, T. A., 2005, "Experimental support for Townsend's Reynolds number similarity hypothesis on rough walls", *Physics of Fluids,* Vol. 17, pp. 035102.

Jimenez, J., 2004, "Turbulent flows over rough walls", *Annual Review of Fluid Mechanics,* Vol. 36, pp. 173–196.

Kim, J., Kim, D., and Choi, H., 2001, "An immersed boundary finite-volume method for simulations of flow in complex geometries", *Journal of Computational Physics,* Vol. 171, pp. 132–150.

Kim, K., Baek, S.-J., and Sung, H. J., 2002, "An implicit velocity decoupling procedure for the incompressible Navier–Stokes equations", *International Journal of Numerical Methods in Fluids,* Vol. 38, pp. 125–138.

Krogstad, P.-Å., and Afros, V., 2012, "About the turbulent statistics in the outer part of a boundary layer developing over two dimensional surface roughness", *Physics of Fluids,* Vol. 24, pp. 075112

Krogstad, P.-Å., and Antonia, R. A., 1999, "Surface roughness effects in turbulent boundary layers", *Experiments in Fluids*, Vol. 27, pp. 450–460.

Krogstad, P.-Å., Andersson, H. I., Bakken, O. M., and Ashrafian, A., 2005, "An experimental and numerical study of channel flow with rough walls", *Journal of Fluid Mechanics*, Vol. 530, pp. 327–352.

Lee, J. H., Seena, A., Lee, S. H., and Sung, H. J., 2012, "Turbulent boundary layers over rod- and cube-roughened walls", *Journal of Turbulence,* Vol. 13, pp. 1–26

Lee, J. H., Sung, H. J., and Krogstad, P.-Å., 2011, "Direct numerical simulation of the turbulent boundary layer over a cube-roughened wall", *Journal of Fluid Mechanics,* Vol. 669, pp. 397–431.

Lee, S. H., and Sung, H. J., 2007, "Direct numerical simulation of the turbulent boundary layer over a rod-roughened wall", *Journal of Fluid Mechanics,* Vol. 584, 125–146.

Lund, T. S., Wu, X., and Squires, K. D., 1998, "Generation of turbulent inflow data for spatially developing boundary layer simulation", *Journal of Computational Physics,* Vol. 140, pp. 233–258.

Mathis, R., Hutchins, N., and Marusic, I., 2009, "Large-scale amplitude modulation of the small-scale structures in turbulent boundary layers", *Journal of Fluid Mechanics,* Vol. 628, pp. 311–337.

Raupach, M. R., Antonia, R. A., and Rajagopalan, S., 1991, "Rough-wall turbulent boundary layers", *Applied Mechanics Reviews,* Vol. 44, pp. 1–25.

Schlatter, P., and Örlü, R., 2010, "Quantifying the interaction between large and small scales in wall-bounded turbulent flows: *a* note of caution", *Physics of Fluids,* Vol. 22 (5), pp. 051704.

Schultz, M. P., and Flack, K. A., 2007, "The rough-wall turbulent boundary layer from the hydraulically smooth to fully rough regime", *Journal of Fluid Mechanics,* Vol**.** 580, pp. 381–405

Shockling, M. A., Allen, J. J., and Smits, A. J., 2006, "Roughness effects in turbulent pipe flow", *Journal of Fluid Mechanics,* Vol. 564, pp. 267–285.

Townsend, A. A., 1976, "*The Structure of Turbulent Shear Flow"*, Cambridge University Press.

Volino, R. J., Schultz, M. P., and Flack, K. A., 2009, Turbulence structure in a boundary layer with two-dimensional roughness", *Journal of Fluid Mechanics,* Vol. 635, pp. 75–101.

Volino, R. J., Schultz, M. P., and Flack, K. A., 2011, "Turbulence structure in boundary layers over periodic two- and three-dimensional roughness", *Journal of Fluid Mechanics*, Vol. 676, pp. 172–190.